Journal of Statistical Physics, Vol. 65, Nos. 3/4, 1991

Externally Perturbed Unstable Systems

H. A. Posch,[1] Heide Narnhofer,[2] and W. Thirring[2]

Received May 2, 1991

We discuss computer solutions of Newton's equations of motion for unstable systems in a container with time-dependent walls. An expansion leads to the formation of a cluster and a significant increase of the temperature. The question of entropy increase for expansion and compression of the system and the related problem of the feasibility of a perpetum mobile of the second kind are investigated.

KEY WORDS: Unstable systems; cluster formation; passivity; computer simulation; second law of thermodynamics.

1. INTRODUCTION

It is generally believed that at the big bang the universe was in thermal equilibrium, but today the interior of stars is about 10^7 K, whereas the interstellar space is only 3 K. It seemingly contradicts our ideas of thermal equilibrium that such vast temperature differences can develop. In previous publications[1-3] we have suggested that this phenomenon is a consequence of the negative specific heat of thermodynamically unstable systems. Classical particles with attractive forces show this feature and numerical solutions of the equations of motion have revealed that such systems developed hot clusters out of homogeneous states.[3-5] In this paper we report the results of computer simulations which include another feature of the history of the universe, namely its expansion and ultimate contraction. The computer solution of Newton's equation of motion shows exactly the surprising features mentioned at the beginning. We start with a hot homogeneous state which does not change with time. Upon expansion the system does some work so that its energy decreases. In this way it comes

[1] Institut für Experimentalphysik, Universität Wien, A-1090 Vienna, Austria.
[2] Institut für Theoretische Physik, Universität Wien, A-1090 Vienna, Austria.

0022-4715/91/1100-0555$06.50/0

into the region of negative specific heat and the homogeneous state is not stable any more. A hot cluster containing a good fraction of all particles is formed. If we stop the expansion, this cluster eventually heats the surrounding gas (Boltzmann's heat death). If we subsequently contract the system, the cluster is evaporated again, but once the original volume is reached, the total energy is higher than at the beginning. This means that work has to be done on the system: even unstable systems do not act as a perpetuum mobile of the second kind.

It is sometimes suggested that the entropy will decrease when the universe eventually contracts. When discussing this issue in our Newtonian model, we have to note the following facts:

(a) We are dealing with a Hamiltonian system and thus the total entropy (Gibbs entropy) $S = -\int d\Omega_N \rho^{(N)} \ln \rho^{(N)}$ is a constant even if the confining potential is time dependent. Here, $\rho^{(N)}$ is the density in the N-particle phase space, and $d\Omega_N$ is the volume element.

(b) If we study an individual orbit, we are in a pure state ($\rho^{(N)}$ is a δ-function) and $S = -\infty$. To get something meaningful we have to introduce a finite grain size in phase space. The Boltzmann entropy $S_B = -\int d\Omega_1 \rho^{(1)} \ln \rho^{(1)}$ is obtained by reducing $\rho^{(N)}$ to $\rho^{(1)}$, the one-particle density in the one-particle phase space. These reduced entropies can change with time, but they can increase or decrease [Remark 3 following Eq. (A6)]. We have reduced this $\rho^{(1)}(\mathbf{x}, \mathbf{p})$ further to the configuration and momentum space. The corresponding x- and p-entropies (S_{Bx} and S_{Bp}) show the following time dependence. When a cluster develops, S_{Bx} decreases, since the spatial density becomes more concentrated. On the other hand, S_{Bp} increases, since the cluster becomes hotter. In fact, the formation of the cluster sets in when the latter effect dominates the former, and the total one-particle entropy increases upon the formation of a cluster. S_{Bx} and S_{Bp} can be considered as special coarse grainings, and thus the question of whether the entropy increases or decreases depends on the kind of coarse graining one chooses. In particular, S_{Bp} decreases upon contraction, since kinetic energy is used up for the evaporation of the cluster. (An analogous effect for stable systems has been predicted by Jaynes.[7]) However, if in the contracted system the original volume has been regained, the total one-particle entropy is higher than at the beginning. Thus, with the provisions mentioned above, we cannot see any support for the speculation of entropy decrease at the big crunch.

In the computer simulations reported here a smooth short-range potential $v \sim -e^{-x^2}$ was used. However, the effects studied do not depend on the detailed form of the potential. This has been shown in another study

(to be published separately) by employing a smoothed potential $v \sim -1/(x^2+\sigma^2)^{1/2}$. As expected, there is no qualitative difference as far as the effects studied in this paper are concerned. The long-range case shows some additional collective phenomena. Their study requires systems with a much larger number of particles and, hence, more computer time.

2. COMPUTER SIMULATION OF CLUSTERING PHASE TRANSITION

We consider a system of N attractively interacting classical point particles confined to a container with (possibly moving) walls of volume $V(t) \in \mathbf{R}^d$. The Hamiltonian is written as

$$\begin{aligned} H_N &= \sum_{i=1}^{N} \frac{\mathbf{p}_i^2}{2m} + \Phi(\mathbf{X}_N) + W(\mathbf{X}_N, t) \\ \Phi(\mathbf{X}_N) &= -\kappa \sum_{i=1}^{N-1} \sum_{j=i+1}^{N} v(\mathbf{x}_i, \mathbf{x}_j) \end{aligned} \tag{2.1}$$

where $\mathbf{X}_N = (\mathbf{x}_1, \mathbf{x}_2, ..., \mathbf{x}_N)$ is a point in N-particle configuration space, and $\mathbf{x}_i \in V(t)$. Here $W(\mathbf{X}_N, t)$ is the purely repulsive interaction energy with the walls of the container. In the following only two-dimensional systems are considered, $d=2$, with the volume $V = L^2$ a square. This restriction is for purely economic reasons and constitutes no serious limitation: all the results apply to higher-dimensional systems as well.

To make contact with previous work, we consider three models for the pair potential v:

A: Gaussian model[3-5,8]

$$v(\mathbf{x}, \mathbf{y}) = e^{-(\mathbf{y}-\mathbf{x})^2/\sigma^2} \tag{2.2}$$

B: Multiple-cell model[2,4,6]

$$v(\mathbf{x}, \mathbf{y}) = \sum_{j=1}^{M} \chi_{V_j}(\mathbf{x})\, \chi_{V_j}(\mathbf{y}) \tag{2.3}$$

where the V_j are a partition of the volume V into M cells, $\bigcup_j V_j = V$, $V_i \cap V_j = \delta_{ij} V_j$, and the characteristic function

$$\chi_{V_j}(\mathbf{x}) = \begin{cases} 1, & \mathbf{x} \in V_j \\ 0, & \mathbf{x} \notin V_j \end{cases}$$

C: Single-cell model[1,3,9]

$$v(\mathbf{x}, \mathbf{y}) = \chi_{V_0}(\mathbf{x})\, \chi_{V_0}(\mathbf{y}), \qquad V_0 \subset V \tag{2.4}$$

In the following, reduced units will be used for which the particle mass m and the potential parameters κ and σ are unity.

In the cell models B and C, which constitute a discretization of the continuous Gaussian model A, the partition function may be evaluated exactly, yielding an analytic expression for the equilibrium temperature T as a function of the total energy E of the system. To demonstrate this relationship, we introduce reduced energy and temperature parameters by

$$e = 1 + \frac{2E}{N(N-1)\kappa} \tag{2.5}$$

$$\Theta = \frac{4K}{dN^2\kappa} = \frac{2k_B T}{N\kappa} \tag{2.6}$$

where the dimension $d=2$, and k_B is Boltzmann's constant (set to unity by an appropriate choice of the temperature scale). K is the kinetic energy. The relation $\Theta(e)$ as computed from the cell models B and C is shown by the dashed curve in Fig. 1 ($N=400$, $M=1600$). The discontinuity at the transition energy $e=e_t^c=1.0024$ indicates a phase transition between a homogeneous gaseous phase ($e>e_t^c$) and a clustered phase ($e<e_t^c$). For the latter the slope of $\Theta(e)$ is negative, indicating a *negative* microcanonical specific heat c_V. Only for such small energies $e<0.4$ (off the scale of Fig. 1) does this slope become positive again, signaling "normal" behavior for c_V.[2,4]

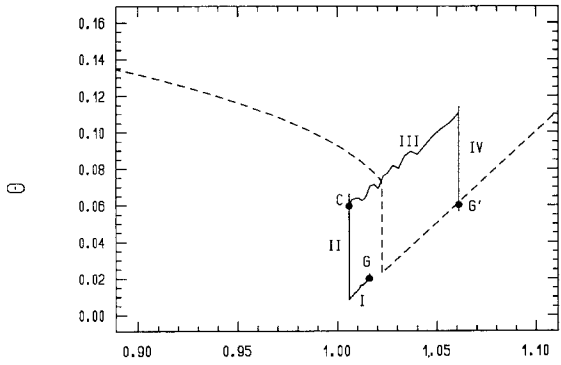

Fig. 1. Plot of the reduced temperature Θ [defined in (2.6)] versus the energy parameter e [defined in (2.5)]. The dashed curve connects all (analytical) equilibrium states for the multiple-cell model B. For $e=e_t^c=1.024$ a phase transition occurs between a clustered phase ($e<e_t^c$) and a homogeneous phase ($e>e_t^c$). The full curve traces the state variations during the cyclic process for the simulated Gaussian model A as outlined in the text. The four stages of the simulation are marked. Full dots indicate equilibrium states.

In the clustered phase a significant amount of all available particles are contained in the cluster. Its spatial extension is small enough to fit into a single small subvolume $V_0 \subset V$. Instead of introducing a whole partition of the volume V into M cells as in model B, it is sufficient to consider a single subvolume V_0. In this sense model C, which was historically first, is a simplified version of model B yielding identical results. If N_c denotes the number of particles in V_0, a cell-model estimate for N_c gives $N_c \sim 2N/\ln(V/V_0)$. Taking $V_0 = \sigma^d$, $\sigma = 1$ being the range of the potential, one finds $N_c \sim 120$ for $N = 400$ particles. This number agrees surprisingly well with computer-simulation results reported below ($N_c \sim 140$).

The continuous potential (2.2) of the Gaussian model A is of short range and free of singularities. It is therefore well suited for numerical simulations using the methods of molecular dynamics. In the past such simulations were carried out to study both the equilibrium[4] and dynamical[3,5] properties of such N-body systems in two dimensions.

In a short film[8] the collapse of an initially homogeneous system onto a cluster containing a considerable fraction, $N_c/N \sim 1/3$, of the available particles and floating in a rest atmosphere formed by the remaining particles may be observed. In all these simulations the system volume V was constant, and periodic (toroidal) boundary conditions were used. Also, the cluster formation in one-dimensional systems has been studied recently.[10]

We have performed a computer simulation of a cyclic process leading from an initial homogeneous equilibrium state through a collapsing phase transition to a collapsed equilibrium state and back again into the homogeneous phase. This is achieved by an adiabatic expansion from an initial volume V to a volume $V_c > V$ for the collapsed system followed by an adiabatic compression to a volume V' identical to the initial volume V. For the evaluation of the work performed by the system on the outside world, periodic boundary conditions are not suitable. Therefore, repulsive boundary conditions are used with the particles confined to a square volume V $(=L^2)$ located symmetrically around the origin:

$$
\begin{aligned}
W(\mathbf{X}_N, t) &= \sum_{i=1}^{N} w(\mathbf{x}_i, t) \\
w(\mathbf{x}, t) &= 10[\xi^2(t) + \eta^2(t)] \\
(\xi, \eta) &= \begin{cases} (|x|, |y|) - \dfrac{s}{2}, & \text{if} \quad |x|, |y| > \dfrac{s}{2} \\ 0, & \text{if} \quad |x|, |y| \leqslant \dfrac{s}{2} \end{cases} \\
\mathbf{x} &= (x, y), \qquad s(t) = L(t) - 2\sigma
\end{aligned}
\tag{2.7}
$$

The expansion (compression) is achieved by moving the cell walls with constant speed $v_L = \frac{1}{2}dL/dt > 0$ (<0), and the rate of work performed by the system

$$\dot{A} = -\frac{\partial W(\mathbf{X}_N, t)}{\partial(L/2)} v_L > 0 \quad (<0) \tag{2.8}$$

Equations (2.1), (2.2), and (2.7) completely define the model solved numerically in the following. The equations of motion for $N = 400$ particles in two dimensions ($d = 2$) are integrated with a Gear predictor–corrector algorithm in the N-representation[11] and correct through terms of order Δt^3. A time step $\Delta t = 0.0025$ was used conserving the total energy to within 0.01 % for isochoric simulation runs of 4 million time steps.

To carry through this cyclic perturbation a homogeneous equilibrium state G must be prepared serving as initial condition for the simulation. In a first step all N particles are distributed randomly over the square volume $V = 800$. The velocity components v_α are taken as equally distributed in $-v_0 < v_\alpha < v_0$, $v_0 = [3K(0)/Nm]^{1/2}$, and $K(0) = 1600$ is the initial kinetic energy. Starting from this initial condition, the system reaches equilibrium within 1000 time units (=400,000 time steps) keeping V and E constant. A snapshot of this equilibrated configuration G is depicted in Fig. 2a.

For the completion of the cyclic process, four computational stages are required:

Stage I. Expansion ($1000 < t < 1200$): During this stage the box size L is increased linearly in time increasing the volume to $V_c = L_c^2 = 2000$. The total energy decrease of the system is

$$E_c - E = -\int_I \dot{A}\, dt < 0$$

pushing the system below the transition energy E_t for the collapsing phase transition, $E_c < E_t$. As a consequence, cluster formation sets in. In Fig. 1 the variation of the instantaneous state parameters Θ and e defined in (2.5) and (2.6), respectively, are indicated by the full line with the four stages of the cyclic process appropriately marked. A comparison with the dashed curve linking equilibrium states obtained for cell model B reveals that the transition energy for the simulated Gaussian model A (estimated from Fig. 1 as $e_t \sim 1.01$) is somewhat lower than the cell model result $e_t^c = 1.024$. The homogeneous Gaussian-model state G (Fig. 2a) lies already in the clustering regime for the cell model. In view of the difference of the involved potentials, such a (minor) discrepancy is only to be expected. The variations of the instantaneous kinetic energy $K = \sum_{i=1}^{N} \mathbf{p}_i^2/2$ and the

potential energy Φ with box size $L(t)$ are depicted in Figs. 3a and 3b. Equilibrium states are indicated by dots.

Stage II. Cluster formation and equilibration at constant energy E_c and volume V_c ($1200 < t < 13200$): At the end of stage I the system is far from equilibrium and relaxes only very slowly toward the clustered equilibrium state C. In Fig. 4 the variation of the instantaneous values of the involved energies as a function of t is shown. As inferred from this figure, about 12,000 time units are needed by the system to approach C, the reason being the weak collision cross section associated with the short-ranged potential (2.2). During stage II the temperature in the condensing

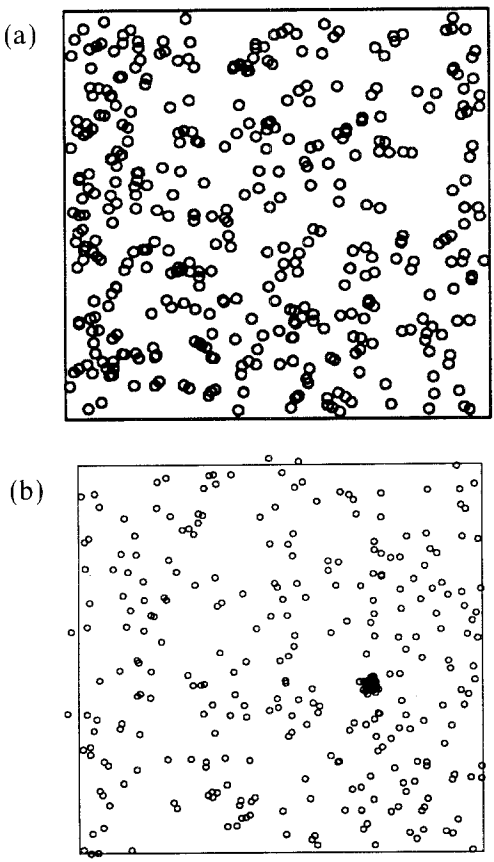

Fig. 2. (a) Snapshot of a homogeneous gaseous configuration G serving as initial condition for the cyclic process. The diameter of the particles is the inflection point of the pair potential (2.2), $D = 1/\sqrt{2}$; the system volume $V = 800$. (b) Snapshot of a clustered state C at the end of the equilibration stage II; $V_c = 2000$.

cluster increases quickly and proportionally to N_c, the number of particles in the cluster, whereas the temperature of the surrounding atmosphere remains much cooler for a long period of time. Only at the end of stage II do these temperatures become equal. The dynamical properties of this cluster formation have been studied in detail in ref. 3. A snapshot of the equilibrated clustered configuration C is depicted in Fig. 2b.

Stage III. Compression ($13{,}200 < t < 13{,}400$): During 200 time units the box size L is decreased linearly in time with speed $-2v_L$, thus

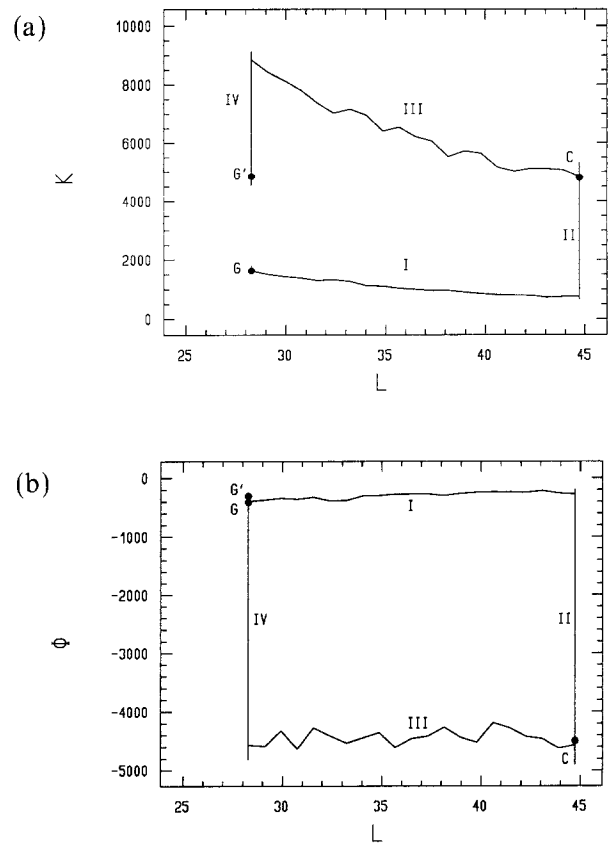

Fig. 3. (a) Instantaneous kinetic energy K as a function of the box size L for the four stages of the simulation distinguished in the text. The four stages are appropriately marked. Full dots indicate equilibrium states. (b) Instantaneous potential energy Φ versus box size L for the cyclic process described in the text. The four stages distinguished in the text are appropriately marked. Full dots denote equilibrium states.

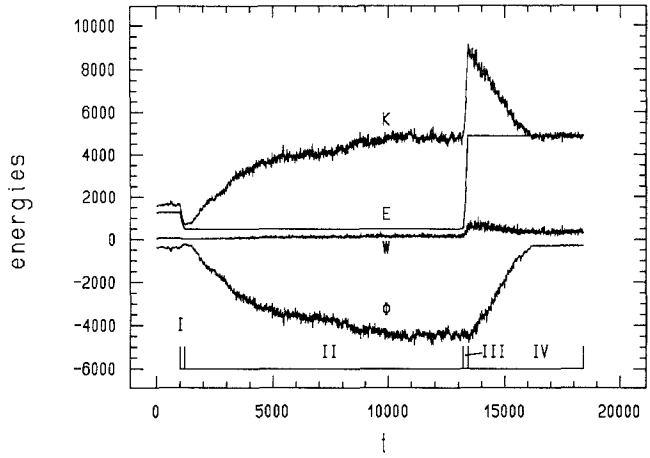

Fig. 4. Variation of the instantaneous values for the kinetic energy K, the potential energy Φ, the interaction energy with the wall W, and the total energy E as a function of time t of the simulation. The four stages distinguished in the text are appropriately marked.

decreasing the system volume back to V again. During this stage $\dot{A} < 0$ and the energy increases to $E' > E_t$. The cluster starts dissolving again.

Stage IV. Cluster dissolution and equilibration at constant energy E' and volume V ($13{,}400 < t < 18{,}400$): The system is left far from equilibrium after stage III and requires considerable time to reach a new homogeneous equilibrium state G' (Fig. 4).

The variation of the instantaneous energies E, Φ, W, and K during all stages of the cyclic process are depicted in Figs. 1, 3, and 4. As expected, the final potential energy is practically identical to its initial value at the start of the cycle. The main result of this numerical exercise is that the total energy E' at the end of the cycle always exceeds its initial value E. The significance of this result and its connection with the second law of thermodynamics will be discussed in Section 4.

3. CALCULATION OF COARSE-GRAINED ENTROPIES

The Gibbs entropy is defined by

$$S = -\int_{\Omega_N} \rho^{(N)}(\Omega_N) \ln \rho^{(N)}(\Omega_N)\, d\Omega_N \tag{3.1}$$

where $d\Omega_N \equiv d^2x_1 \cdots d^2x_N\, d^2p_1 \cdots d^2p_N$, and the N-particle distribution $\rho^{(N)}$ is normalized according to

$$\int \rho^{(N)}(\Omega_N)\, d\Omega_N = 1 \tag{3.2}$$

S is a constant of the motion even in the presence of an external time-dependent perturbation $W(\mathbf{X}_N, t)$ such as in (2.1). If there is anything to be learned from the concept of entropy, reduced distribution functions must be used. The general properties for such reduced entropies are given in Appendix A. In particular, the following inequalities are obtained from (A.5) for a system of N particles:

$$S \leqslant NS_{\mathrm{B}} \leqslant N(S_{\mathrm{B}x} + S_{\mathrm{B}p}) \tag{3.3}$$

Here,

$$S_{\mathrm{B}} = -\int \rho^{(1)}(\Omega_1) \ln \rho^{(1)}(\Omega_1)\, d\Omega_1 \tag{3.4}$$

with

$$\rho^{(1)}(\Omega_1) = \int \rho^{(N)}(\Omega_N)\, d\Omega_{N-1}, \qquad \int \rho^{(1)}(\Omega_1)\, d\Omega_1 = 1$$

is the familiar Boltzmann entropy in the phase space of a single particle, and $d\Omega_{N-k} \equiv d^2x_{N-k+1} \cdots d^2p_N$. The $S_{\mathrm{B}x}$ and $S_{\mathrm{B}p}$ are obtained by further reduction of $\rho^{(1)}$ to the respective coordinate and momentum spaces of a single particle:

$$S_{\mathrm{B}x} = -\int \rho_x^{(1)}(\mathbf{x}_1) \ln \rho_x^{(1)}(\mathbf{x}_1)\, d^2x_1 \tag{3.5}$$

$$S_{\mathrm{B}p} = -\int \rho_p^{(1)}(\mathbf{p}_1) \ln \rho_p^{(1)}(\mathbf{p}_1)\, d^2p_1 \tag{3.6}$$

where

$$\rho_x^{(1)} = \int \rho^{(1)}(\Omega_1)\, d^2p_1, \qquad \int \rho_x^{(1)}\, d^2x_1 = 1$$

$$\rho_p^{(1)} = \int \rho^{(1)}(\Omega_1)\, d^2x_1, \qquad \int \rho_p^{(1)}\, d^2p_1 = 1$$

The first inequality in (3.3) becomes an equality iff $\rho^{(N)}$ factorizes into a product of N one-particle distributions $\rho^{(1)}$.[12] It is demonstrated in

Appendix B that in the thermodynamic limit $N \to \infty$ (with momentum scaling invoked as discussed in detail in Section 3 of ref. 3) this is indeed the case for both the canonical and the microcanonical distributions.

The actual numerical evaluation of S_B, S_{Bx}, and S_{Bp} is complicated by a number of facts which require consideration:

(a) Coarse-grained measures have to be introduced by averaging $\rho^{(1)}$, $\rho_x^{(1)}$, and $\rho_p^{(1)}$ over partitions of their respective spaces.

(b) N is finite, and we are far from the thermodynamic limit. This requires careful assessment of the boundary conditions. For the reflecting boundary conditions of Section 2 and in the thermodynamic limit the cluster would form precisely in the center of the box. In a finite system and in particular in a system with short-range interactions (2.2) the cluster has the freedom to float around this point. The (nonequilibrium) entropies estimated from a single trajectory therefore lack the proper symmetry. It is argued in Appendix B that this will not affect the numerical results significantly.

(c) $N = 400$ is also too small a number of particles to obtain precise estimates for the (nonequilibrium) single-particle distributions from a single run. Computational costs have prevented us from carrying out the simulation of a whole ensemble of N-particle trajectories—distinguished only by different initial conditions—in parallel. To improve the statistics, we have averaged the distributions over a time interval short compared to the relaxation time (see below).

From this discussion it is obvious that the coarse-grained entropies reported below will obey only the inequalities and not the equalities in (3.3), as is indeed the case. They are calculated for a finite system and for single-particle phase spaces with very rough coarse graining. Their actual numbers are not of too much importance. However, their variation with time is significant, which make them very useful to understand the time evolution of the collapsing systems during the cyclic process of Section 2.

For the numerical evaluation the coordinate space was partitioned into squares of length $\Delta L = \sigma$ requiring 30×30 boxes for the initial and final homogeneous stages and 46×46 boxes for the collapsed stage II. This is a coarse partition allowing most of the particles of the main cluster to be in a single box. For the momenta local isotropy was assumed and p^2 was subdivided into 40 slices of width $\Delta p^2 = 3.6$. Thus, a maximum of 84,640 and 2116 phase-space boxes was used for the evaluation of S_B and S_{Bx}, respectively, whereas only 40 boxes sufficed for S_{Bp}. Altogether 400 instantaneous N-particle configurations each separated by $10\Delta t$ were used for the calculation of the coarse-grained densities. Each entropy value is

actually an average over 10 time units of the trajectory. In view of the very long relaxation times, this procedure is adequate. The method therefore determines the coarse-grained densities essentially from the time duration the particles spend in the various partitions of the single-particle phase space.[13]

The result for the cyclic process is shown in Fig. 5 as a function of time. The following remarks are in order:

(a) $S_B < S_{Bx} + S_{Bp}$ at any time, in accordance with the discussion following (3.3).

(b) The noise for the entropies S_B and S_{Bx} involving spatial distributions is considerably larger than that of S_{Bp}. It is caused by the drift of the main cluster over the partition boundaries. The smooth behavior of S_{Bp} even during violent transient stages is a consequence of local equilibrium being established quickly, as observed in ref. 3.

(c) The small drop of S_B (and $S_{Bx} + S_{Bp}$) during the expansion stage I is spurious. It results from an unbalanced treatment of configuration and momentum spaces by the (arbitrary) partitioning procedure, and should be disregarded.

(d) As expected, the time dependence of the momentum entropy S_{Bp} closely reflects that of the kinetic energy K in Fig. 4. Whenever the temperature goes down—such as during expansion in stage I—also S_{Bp} strongly decreases. Any temperature increase is accompanied by an increase of S_{Bp}.

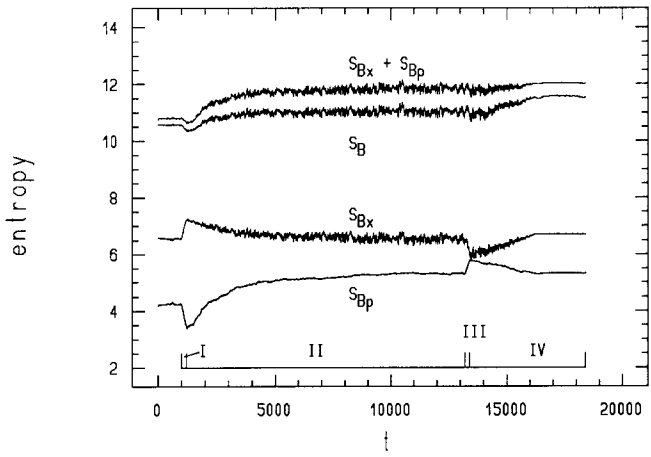

Fig. 5. Coarse-grained entropies as a function of time: S_B is the Boltzmann entropy, S_{Bx} and S_{Bp} are space and momentum entropies as described in the text.

(e) During equilibration in stage II the spatial entropy S_{Bx} decreases significantly. This is due to the formation of the main cluster whose particles occupy essentially a single box in coordinate space. Similarly, S_{Bx} increases in stage IV when the cluster dissolves again. The final equilibrium value of S_{Bx} agrees with its initial equilibrium value.

(f) Whether an arbitrary reduced entropy increases or decreases in a nonequilibrium situation depends very much on the space on which it is defined. Thus, S_{Bx}, depending solely on position variables, decreases during the cluster formation, whereas the complementary S_{Bp}, depending on momentum variables, increases. The full Boltzmann entropy S_B increases only slightly.

(g) The net effect of the complete cyclic process is a (slight) increase of S_B in accordance with the second law. This increase is solely due to the increase of S_{Bp} and is reflected by the increase of the system's kinetic energy K.

4. PASSIVITY

We have seen that the entropy is not very useful for discussing the irreversible features of our system. The Gibbs entropy is constant [even with an external time-dependent potential $W(x, t)$] and the coarse-grained entropies may increase or decrease. The observer-independent fact seems to be the passivity of the system, which means that after a period τ of $W(x, t)$ the system ends up with a higher energy than at $t=0$: it has to be worked on rather than doing work. To ease the notation, unnecessary indices and boldface vector characterization are omitted in this section. For example, $H^{(N)}$ and $W(\mathbf{X}^{(N)}, t)$ are written as H and $W(x, t)$, respectively.

Remarks:

1. The notion of passivity has been introduced by Pusz and Woronowicz.[14,15] In their celebrated paper they showed that the KMS (=equilibrium) states are characterized by their passivity against all periodic perturbations $W(t)$. We are concerned with a somewhat different question, namely, which orbits of pure states are passive for a given W, and which are not?

2. Passivity is equivalent to the statement that the system cannot be used as a perpetuum mobile of the second kind. Suppose that at the end of the cycle the energy E of the system has been changed to $E' > E$ (or $E' < E$). To restore the initial energy E, we have to extract (or feed in) heat, and by doing so we will end up at some random point of this particular energy shell. If the orbits with $E' > E$ (or $E' < E$) dominate the

volume of the energy shell, we can repeat the process with the same outcome, and in the first case the system will consume work and produce heat. In the second case it is the other way around and we have a perpetuum mobile of the second kind. Thus, the impossibility of the latter is equivalent to the condition that most orbits are passive ($E' > E$).

In our situation the reason for passivity is intuitively clear, since the gas is still cold at the expansion phase I and hot at the compression phase III. Thus, the pressure on the wall is less during expansion than during compression. Nevertheless, one immediately is haunted by the following question: Choosing $t=0$ appropriately, our $W(x, t)$ is an even function of t, $W(x, t) = W(x, -t)$. As a consequence, the transformation ϑ: $(x_i, p_i) \to (x_i, -p_i)$ reverses the motion and preserves the volume $d\Omega$ of phase space: $\alpha_{-t} = \vartheta \circ \alpha_t \circ \vartheta$. Thus, one may assert that there are just as many points in phase space with passive orbits $[E(\tau) > E(0)]$ as with active orbits $[E(\tau) < E(0)]$, τ being the period of the cycle. Nevertheless, picking random initial conditions, we always get passive orbits and never stumble on active orbits. We shall devote this section to the resolution of this (apparent) paradox, since it shows to what extent a perpetuum mobile of the second kind is impossible. To our knowledge this problem has never been discussed in the light of passivity.

Now, $H + W(x, t)$, $W(x, t+\tau) = W(x, t) = W(x, -t)$, induces a family of measure-preserving transformations α_t in phase space Ω which carries H into $H \circ \alpha_t$. Denote the passive (resp. active) sets $\mathscr{S}_{p,a}(\alpha_\tau) = \{z \in \Omega: H(z) \lesseqgtr H \circ \alpha_\tau(z)\}$. Since H is invariant under ϑ, we see that $\vartheta \circ \alpha_t(\mathscr{S}_p) = \mathscr{S}_a$:

$$H(z) = H \circ \alpha_\tau^{-1} \circ \alpha_\tau(z) = H \circ \vartheta \circ \alpha_\tau \circ \vartheta \circ \alpha_\tau(z) = H \circ \alpha_\tau(\vartheta \circ \alpha_\tau(z)) \tag{4.1}$$

Since $H \circ \alpha_\tau(z) = H \circ \vartheta \circ \alpha_\tau(z)$, we note

$$H(z) \lesseqgtr H \circ \alpha_\tau(z) \Leftrightarrow H \circ \alpha_\tau(\vartheta \circ \alpha_\tau(z)) \lesseqgtr H(\vartheta \circ \alpha_\tau(z)) \tag{4.2}$$

such that

$$\mathscr{S}_a(\alpha_\tau) = \vartheta \circ \alpha_\tau(\mathscr{S}_p(\alpha_\tau))$$

Since $\vartheta \circ \alpha_\tau$ is a measure-preserving bijection, this proves our assertion. Thus, if for a given energy shell $\mathscr{S}_E = \{z \in \Omega: H(z) = E\}$ the measure of its points $\in \mathscr{S}_p$ which at the time τ have an energy $E' > E$ is $\mu(E, E')$, then the measure of the active points of $\mathscr{S}_{E'}$ which after τ have the energy $E < E'$ is exactly the same, $\mu(E, E') = \mu(E', E)$:

$$\begin{aligned} \mu(E, E') &= \int d\Omega\, \delta(H - E)\, \delta(H \circ \alpha_\tau - E') \\ &= \int d\Omega\, \delta(H \circ \vartheta - E)\, \delta(H \circ \alpha_\tau^{-1} \circ \vartheta - E') \\ &= \int d\Omega\, \delta(H \circ \alpha_\tau - E)\, \delta(H - E') \end{aligned} \tag{4.3}$$

since ϑ and α_τ are measure-preserving bijections. However, the measure of $\mathscr{S}_E$ increases rapidly with E and the measure μ_p of all passive points with energy below E_0 will dominate the measure μ_a of the active points. Taking $H \geqslant 0$, we have

$$\mu_a = \int_0^{E_0} dE \int_0^{E} dE'\, \mu(E, E')$$

and

$$\begin{aligned}\mu_p &= \int_0^{E_0} dE \int_E^{\infty} dE'\, \mu(E, E') \\ &= \int_0^{E_0} dE \int_E^{E_0} dE'\, \mu(E, E') + \int_0^{E_0} dE \int_{E_0}^{\infty} dE'\, \mu(E, E') \\ &= \mu_a + \int_0^{E_0} dE \int_{E_0}^{\infty} dE'\, \mu(E, E') \qquad (4.4)\end{aligned}$$

The more the last integral exceeds μ_a, the less likely it is that one will find passive points below a given energy E_0. The explicit evaluation of $\mu(E, E')$ for our system is beyond our means. However, at the risk of making this paper bulky, we shall study these phenomena at a simple example where everything can be evaluated analytically.

Example 4.1. We start with one particle in one dimension and replace the wall potential by a harmonic potential. For the expansion and compression phase we make the sudden approximation and take

$$H = \frac{p^2}{2} + W(x, t), \qquad W(x, t) = \begin{cases} \dfrac{\omega^2}{2} x^2 & \text{for } |t| < \dfrac{\tau}{4}, \\ \dfrac{1}{2} x^2 & \text{for } \dfrac{\tau}{4} \leqslant t \leqslant \dfrac{\tau}{2}, \end{cases} \qquad \omega > 1$$

and $W(x, t) = W(x, -t)$, $W(x, t+\tau) = W(x, t)$. Thus, at the expanded phase the motion is on the circles $p^2 + x^2 = 2E$ and in the compressed phase on ellipses $p^2 + \omega^2 x^2 = 2E'$ (Fig. 6). If at the compression time $t = -\tau/4$ we have $p = 0$, then the particle will move outside the circle $p^2 + x^2 = 2E$ till $t = \tau/4$ and we shall have $p^2(\tau/4) + x^2(\tau/4) \equiv 2E' > 2E$. On the other hand, if $x(-\tau/4) = 0$, the ellipse is inside the circle and $p^2(\tau/4) + x^2(\tau/4) \equiv 2E' < 2E$. After expansion at time $t = \tau/2$ the particle moves on a circle $p^2 + x^2 = 2E'$, and the total change of energy during a full cycle of the potential W with period τ is $\delta E = E' - E$. To draw the borderline

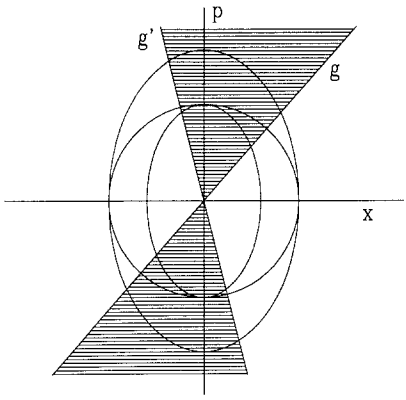

Fig. 6. Phase space for the periodically perturbed harmonic oscillator in Example 4.1. The straight lines g: $p=(-\gamma+(\gamma^2+1)^{1/2})\,\omega x$ and g': $p=(-\gamma-(\gamma^2+1)^{1/2})\,\omega x$, $\gamma=\cot\omega\tau/2$, separate active and passive regions. Active regions are shaded.

between the active and the passive regions, we recall that the time development for $t=-\tau/4$ to $t=\tau/4$ is

$$(x,\,p)\to\left(x\cos\frac{\omega\tau}{2}+\frac{p}{\omega}\sin\frac{\omega\tau}{2},\;-\omega x\sin\frac{\omega\tau}{2}+p\cos\frac{\omega\tau}{2}\right)$$

where $(x(-\tau/4),\,,\,p(-\tau/4)\equiv(x,\,p))$. The change of energy

$$\delta E=\frac{1}{2}\left[p^2\left(\frac{\tau}{4}\right)+x^2\left(\frac{\tau}{4}\right)-p^2-x^2\right]=\frac{1}{2}\left(1-\frac{1}{\omega^2}\right)\left[p^2\left(\frac{\tau}{4}\right)-p^2\right]$$

$$=\frac{1}{2}\left(1-\frac{1}{\omega^2}\right)\left[(x^2\omega^2-p^2)\sin^2\frac{\omega\tau}{2}-2px\omega\sin\frac{\omega\tau}{2}\cos\frac{\omega\tau}{2}\right]$$

δE vanishes on the lines $p=\omega x[-\gamma\pm(\gamma^2+1)^{1/2}]$, $\gamma=\cot\omega\tau/2$. The regions closer to the p axis are active (the shaded region in Fig. 6), the complementary ones are passive. The circle $p^2+x^2=2E$ is dominated by passive regions if $\alpha>\pi/2$ (Fig. 6), which is always true irrespective of γ (that is, τ), as the scalar product of the boundary vectors is negative:

$$\begin{pmatrix}\omega(-\gamma+(\gamma^2+1)^{1/2})\\ 1\end{pmatrix}\cdot\begin{pmatrix}\omega(-\gamma-(\gamma^2+1)^{1/2})\\ 1\end{pmatrix}=1-\omega^2<0$$

Observe that δE has a factor $(1-1/\omega^2)$. So the same conclusion holds for $\omega<1$, which means that also the energy of the expanded phase is likely to increase.

So far we have seen that in the simple example, on each energy shell the active regions are smaller than the passive ones. Actually we want much more for the physical systems in the thermodynamic limit: the active region should be completely negligible. This is a typical feature of the thermodynamic limit $N \to \infty$, where usually the volume of the energy shell obeys

$$\int_0^\infty dE'\, \mu(E, E') \to e^{N\sigma(\varepsilon)}$$

Here, σ is the entropy per particle, and $\varepsilon = E/N$. Thus, one expects an exponential dependence of $\mu(E, E')$ on N, and in the limit $N \to \infty$ the ratio $\mu_a(N\varepsilon)/\mu_p(N\varepsilon) \to e^{-Nf(\varepsilon)}$ with $f > 0$. We shall not attempt to demonstrate this claim for the unstable system studied in this paper because we believe that the considerations of this section are more general and apply to stable and unstable systems alike. The reason for this seems to be that the energy is semibounded from below. This offers far more possibilities for absorbing energy than for giving energy off and makes the physical systems passive. For the sake of completeness we calculate $\mu(E, E')$ explicitly for N noninteracting harmonic oscillators subjected to the same external periodic perturbation as in the preceding example.

Example 4.2. We have

$$H = \sum_i \left[\frac{p_i^2}{2} + W(x_i, t) \right]$$

$W(x, t)$ is from Example 4.1. To evaluate (4.3), we observe that

$$H \circ \alpha_\tau = \tfrac{1}{2}(ap^2 + 2bxp + cx^2) = \tfrac{1}{2} z' M z$$

with $z' = (p, x)$, $z = \binom{p}{x}$, and

$$a = \cos^2 \frac{\omega\tau}{2} + \frac{1}{\omega^2} \sin^2 \frac{\omega\tau}{2}, \qquad b = \left(\frac{1}{\omega} - \omega \right) \cos \frac{\omega\tau}{2} \sin \frac{\omega\tau}{2}$$

$$c = \cos^2 \frac{\omega\tau}{2} + \omega^2 \sin^2 \frac{\omega\tau}{2}$$

The matrix

$$M = \begin{pmatrix} a & b \\ b & c \end{pmatrix}$$

is measure preserving and thus $\det M = 1$. Its eigenvalues are m and $1/m$, with

$$m = \frac{a+c}{2} + \left[\left(\frac{a+c}{2}\right)^2 - 1\right]^{1/2}$$

Introducing the integral representation for the δ-function, we find for even N [$\Theta(x)$ is the step function $=1$ for $x>0$, $=0$ otherwise]

$$\begin{aligned}
\mu(E, E') &= \int d^{2N}z\, \delta\left(\sum_{j=1}^{N} \frac{1}{2} z_j^2 - E\right) \delta\left(\sum_{j=1}^{N} \frac{1}{2} z_j M z_j - E'\right) \\
&= \int_{-\infty}^{\infty} \frac{ds\, dt}{(2\pi)^2} \int \exp\left[is\left(\sum_{j=1}^{N} \frac{1}{2} z_j^2 - E\right)\right. \\
&\quad \left. + it\left(\sum_{j=1}^{N} \frac{1}{2} z_j M z_j - E'\right)\right] d^{2N}z \\
&= \lim_{\varepsilon \downarrow 0} \int_{-\infty}^{\infty} \frac{ds\, dt}{(2\pi)^2} e^{-i(sE + tE')} \left(\frac{2\pi}{s + tm + i\varepsilon}\right)^{N/2} \left(\frac{2\pi}{s + t/m + i\varepsilon}\right)^{N/2} \\
&= \lim_{\varepsilon \downarrow 0} \frac{1}{m - 1/m} \int_{-\infty}^{\infty} \frac{dv\, du (2\pi)^N/(2\pi)^2}{(u + i\varepsilon)^{N/2}\, (v + i\varepsilon)^{N/2}} \\
&\quad \times \exp\left[-iv \frac{m^2 E - mE'}{m^2 - 1} - iu \frac{mE' - E}{m^2 - 1}\right] \\
&= \frac{m}{m^2 - 1} \frac{(2\pi)^N}{[(N/2 - 1)!]^2} \Theta(Em - E')\, \Theta(E'm - E) \\
&\quad \times (E - mE')^{N/2 - 1}\, (E' - mE)^{N/2 - 1} \frac{m^{N/2 - 1}}{(m^2 - 1)^{N-2}}
\end{aligned}$$

To arrive at this result, we first used the formula for Gaussian integrals and then applied the residue theorem. This function has its maximum for $E'_m = [(1 + m^2)/2m]E > E$ and thus the passive region $E' > E$ is favored. In fact,

$$\frac{\mu(E, E'_m)}{\mu(E, E)} = \left(\frac{1 + m}{2\sqrt{m}}\right)^{N-2}$$

and since $(1 + m)/2 > \sqrt{m}$, this ratio increases exponentially with N.

5. CONCLUSIONS

The computer simulation verified our conjecture that the expansion of a gas of particles with unstable interactions leads to hot clusters. The

difference from stable interactions is that in the latter case the condensed phase remains at the same temperature. Conversely, by compression the temperature first increases, but then decreases again due to the evaporation of the clusters. Nevertheless, at the end of a complete expansion–compression cycle the total energy is higher than at the beginning, which also leads to a net increase of the entropy. The increase of energy in a cyclic process which is not completely adiabatic has been named passivity and seems to be a key feature of many-body systems. In a simple model we found that below a fixed energy shell for each particle the fraction f of the volume in phase space which is not passive is $<50\%$. Thus, for a many-particle system $[f/(1-f)]^N \to 0$ for $N \to \infty$. Since the phase space in this case is simply a product of spaces such as Fig. 6, the *active* regions of phase space violating the second law of thermodynamics are similar to a Cantor set in the thermodynamic limit. Their relative volume goes to zero. A similar result has been obtained recently for *finite* systems in nonequilibrium steady states for which the accessible phase space shows a multifractal structure.[16,17] The volume occupied by states violating the second law vanishes also in this case.

APPENDIX A. REDUCED ENTROPIES

Let $\rho(z)$, $\rho_1(z)$ be probability distributions over the phase space $\Omega \ni z$. The basic fact is the positivity of the relative entropy

$$S(\rho_1 \mid \rho) := \int d\Omega\, \rho(\ln \rho - \ln \rho_1) \geqslant 0 \tag{A.1}$$

This follows from $\int d\Omega\, \rho = \int d\Omega\, \rho_1 = 1$ and the inequality $\ln x \geqslant 1 - 1/x$. If ρ_1 is of the canonical form

$$\rho_1(z) = \exp[-\beta H(z) + \beta \langle H \rangle_{\rho_1} - S(\rho_1)]$$

where

$$\langle H \rangle_{\rho_1} = \int d\Omega\, \rho_1(z)\, H(z)$$

and

$$S(\rho_1) = -\int d\Omega\, \rho_1(z) \ln \rho_1(z)$$

then (A.1) implies

$$0 \leqslant S(\rho_1) - S(\rho) - \beta \langle H \rangle_{\rho_1} + \beta \langle H \rangle_{\rho} \tag{A.2}$$

(A.2) is the general form of the variational principle, which says that among the densities ρ with expectation value of H less than or equal to $\langle H\rangle_{\rho_1}$ the canonical ρ_1 has the highest entropy. Conversely, one can say that among the densities with entropy $\geqslant S(\rho_1)$ the canonical ρ_1 gives the lowest expectation value of H.

If Ω is a product space, $z=(x, y)$, $d\Omega = dx\,dy$ and we define reduced densities $\rho_1(x)=\int dy\,\rho(x, y)$, $\rho_2(y)=\int dx\,\rho(x, y)$, and $\rho_{12}(x, y)=\rho_1(x)\,\rho_2(y)$, then $S(\rho_{12}\mid\rho)\geqslant 0$ implies the subadditivity

$$S(\rho)\leqslant S(\rho_{12})=S(\rho_1)+S(\rho_2) \tag{A.3}$$

If, in addition, ρ is canonical $\sim e^{-\beta H}$ we have bounds on both sides

$$\begin{aligned} 0\leqslant S(\rho_1)+S(\rho_2)-S(\rho)&\leqslant \beta\langle H\rangle_{\rho_{12}}-\beta\langle H\rangle_{\rho}\\ &=\beta\int dx\,dy\,H(x, y)[\rho_1(x)\,\rho_2(y)-\rho(x, y)] \end{aligned} \tag{A.4}$$

Remarks:

1. In (A.1) equality holds iff $\rho=\rho_1$, since $\ln x>1-1/x$ unless $x=1$.

2. If $\rho_1(x)\geqslant\rho(x, y)$ and thus $-\ln\rho(x, y)\geqslant -\ln\rho(x)$, $\forall y$, then we get the monotonicity $S(\rho)\geqslant S(\rho_1)$. For discrete measures this is always satisfied.

3. (A.3) obviously generalizes if Ω is an N-fold product $z=(x_1, x_2,..., x_N)$. In particular, if ρ is symmetric,

$$S(\rho)\leqslant NS(\rho_1) \tag{A.5}$$

with $=$ iff $\rho(x_1,..., x_N)=\prod_{j=1}^{N}\rho_1(x_j)$.

Inequalities in both directions can be inferred by the following general consideration.

If we fix the expectation value of some observables A_i, $\int dz\,\rho(z)\,A_i(z)=a_i$, among such ρ's the one with the highest entropy is

$$\rho_1(z)=\exp\left[-\sum_i \beta_i A_i(z)\right]\Big/\int d\Omega'\exp\left[-\sum_j \beta_j A_j(z')\right]$$

The β_i are to be chosen such that $\int d\Omega\,\rho_1(z)\,A_i(z)=a_i$. This optimal property is again a consequence of (A.1):

$$\begin{aligned} &0\leqslant S(\rho_1\mid\rho)\\ &=\int d\Omega\,\rho(z)\left[\ln\rho(z)+\sum_i\beta_i A_i(z)\right]+\ln\int d\Omega'\exp\left[-\sum_j\beta_j A_j(z')\right]\\ &=-S(\rho)+S(\rho_1) \end{aligned}$$

If ρ is also of the canonical form $\sim e^{-\beta H}$, the $S(\rho \mid \rho_1) \geqslant 0$ supplies the other bound

$$0 \leqslant S(\rho_1) - S(\rho) \leqslant \beta(\langle H \rangle_{\rho_1} - \langle H \rangle_{\rho}) \tag{A.6}$$

In particular, $\langle H \rangle_{\rho_1} = \langle H \rangle_{\rho} \Rightarrow S(\rho_1) = S(\rho)$.

Remarks:

1. (A.2) can be considered as a special case of (A.6) if $i \to (\bar{x}, \bar{y})$, $A_i(-x, y) \to \delta(x - \bar{x})$, and $\delta(y - \bar{y})$, $\sum_i \to \int d\bar{x} + \int d\bar{y}$; $\rho = \rho_1(x)\,\rho_2(y)$ is thus the density with highest entropy, given the reduced densities ρ_1 and ρ_2.

2. All these results generalize directly to the quantum mechanical situation with $\int d\Omega \to \mathrm{Tr}$ and the ρ's become density matrices. Note that for the generalized variational principle (A.6) to hold, it is not necessary to assume that the A_i commute. Also, in the quantum mechanical context (A.4) may be used to determine the accuracy of a one-particle description.

3. In the classical folklore on the subject (see ref. 18) one finds a theorem which states that the entropy of the coarse-grained density (matrix) increases with time. The proof boils down to the following. Let $\bar{\rho}$ be a coarse-graining of ρ which implies $S(\bar{\rho}) \geqslant S(\rho)$. Now evolve ρ (unitarily) with time such that $S(\rho(t)) = S(\rho(0))$. If we take a coarse graining compatible with ρ for $t = 0$, $\bar{\rho}(0) = \rho(0)$, we get

$$S(\bar{\rho}(t)) \geqslant S(\rho(t)) = S(\rho(0)) = S(\bar{\rho}(0))$$

Though mathematically impeccable, the proof cannot be useful. Nothing has been assumed about the unitary time evolution. It could very well be strictly periodic, in which case $S(\bar{\rho})$ has to return to its original value. The flaw in the demonstration is that $\rho(t)$ will not be compatible with coarse graining such that $S(\bar{\rho}(t')) \leqslant S(\bar{\rho}(t))$ for $t' > t$ cannot be excluded.

APPENDIX B. RELEVANCE OF THE BOLTZMANN ENTROPY

We have already noticed that the entropy calculated from the one-particle density, the Boltzmann entropy S_{B}, gives an upper bound to S/N, where S is the N-particle Gibbs entropy. It remains to show that for the equilibrium states of our unstable systems Boltzmann entropy and Gibbs entropy per particle coincide, or equivalently, the reduced n-particle distribution ρ_n factorizes, $n \leqslant N$,

$$\begin{aligned} &\rho_n(\mathbf{X}_n, \mathbf{P}_n) = \rho_1(\mathbf{x}_1, \mathbf{p}_1) \cdots \rho_1(\mathbf{x}_n, \mathbf{p}_n) \\ &\mathbf{X}_n = (\mathbf{x}_1, \ldots, \mathbf{x}_n), \qquad \mathbf{P}_n = (\mathbf{p}_1, \ldots, \mathbf{p}_n) \end{aligned} \tag{B.1}$$

The microcanonical expectation value of a dynamical variable $f(\mathbf{X}_n, \mathbf{P}_n)$ defines ρ_n:

$$\omega(f) = \int \rho_n(\mathbf{X}_n, \mathbf{P}_n)\, f(\mathbf{X}_n, \mathbf{P}_n)\, d\mathbf{X}_n\, d\mathbf{P}_n \tag{B.2}$$

It is obtained from the microcanonical N-body distribution $\rho^{(N)}$ according to

$$\omega(f) = \lim_{N\to\infty} \int \rho_n^{(N)}(\mathbf{X}_n, \sqrt{N}\,\mathbf{P}_n)\, f(\mathbf{X}_n, \mathbf{P}_n)\, d\mathbf{X}_n\, d\mathbf{P}_n \tag{B.3}$$

where an appropriate momentum scaling is required to perform the thermodynamic limit, which is discussed in detail in Section 3 of ref. 3. Neglecting boundary effects ($W=0$), we rewrite the Hamiltonian (2.1)

$$H_N = \sum_{i=1}^{N} \frac{\mathbf{p}_i^2}{2m} + \Phi(\mathbf{X}_N), \qquad \Phi(\mathbf{X}_N) = -\sum_{i=1}^{N-1} \sum_{j=i+1}^{N} \kappa v(\mathbf{x}_i, \mathbf{x}_j)$$

as

$$H_N = \sum_{i=1}^{N} \frac{\mathbf{p}_i^2}{2m} + \Phi(\mathbf{X}_{N-n}) + \sum_{i=1}^{n} \phi(\mathbf{x}_i, \mathbf{X}_{N-n}) + \Phi(\mathbf{X}_n)$$

where

$$\phi(\mathbf{x}_i, \mathbf{X}_{N-n}) = -\kappa \sum_{l=N-n+1}^{N} v(\mathbf{x}_i, \mathbf{x}_l)$$

Insertion of the microcanonical N-particle density into (B.3) yields

$$\omega(f) = \lim_{N\to\infty} c_N \int d\mathbf{X}_N\, d\mathbf{P}_N\, f(\mathbf{X}_n, \mathbf{P}_n) \times \delta\left[\sum_{i=1}^{N} \frac{N\mathbf{p}_i^2}{2m} + \Phi(\mathbf{X}_n) + \Phi(\mathbf{X}_{N-n}) + \sum_{i=1}^{n} \phi(\mathbf{x}_i, \mathbf{X}_{N-n}) - E_N\right]$$

The normalization constant c_N is determined from $\omega(1)=1$. Carrying out $\int d\mathbf{P}_{N-n} = \int \prod_{l=N-n+1}^{N} d^2p_l$, one obtains

$$\omega(f) = \lim_{N\to\infty} c_{N,n} \int d\mathbf{X}_n\, d\mathbf{P}_n\, f(\mathbf{X}_n, \mathbf{P}_n) \int d\mathbf{X}_{N-n} \times \left\{E_N - \Phi(\mathbf{X}_{N-n}) - \Phi(\mathbf{X}_n) - \sum_{i=1}^{n} \left[\frac{N\mathbf{p}_i^2}{2m} + \phi(\mathbf{x}_i, \mathbf{X}_{N-n})\right]\right\}^{N-n-1}$$

The various energy terms scale according to $E_N = \varepsilon N^2$, $\Phi(\mathbf{X}_{N-n}) \sim N^2$, $\phi(\mathbf{x}_i, \mathbf{X}_{N-n}) \sim N$, and $\Phi(\mathbf{X}_n) = O(1)$. Thus,

$$\lim_{N\to\infty} \left(1 - \frac{\sum_{i=1}^{n} [N\mathbf{p}_i^2/2m + \phi(\mathbf{x}_i, \mathbf{X}_{N-n})] + \Phi(\mathbf{X}_n)}{\varepsilon N^2 - \Phi(\mathbf{X}_{N-n})}\right)^{N-n-1}$$

$$= \lim_{N\to\infty} \exp\left\{-\beta(\mathbf{X}_{N-n}) \sum_{i=1}^{n} \left[\frac{\mathbf{p}_i^2}{2m} + \frac{1}{N}\phi(\mathbf{x}_i, \mathbf{X}_{N-n})\right]\right\} \tag{B.4}$$

with

$$\lim_{N\to\infty} \frac{N^2}{\varepsilon N^2 - \Phi(\mathbf{X}_{N-n})} = \lim \beta(\mathbf{X}_{N-n}) \sim O(1) \tag{B.5}$$

This gives

$$\omega(f) = \lim_{N\to\infty} c_{N,n} \int d\mathbf{X}_{N-n} [\varepsilon N^2 - \Phi(\mathbf{X}_{N-n})]^{N-n-1} \int d\mathbf{X}_n \, d\mathbf{P}_n \, f(\mathbf{X}_n, \mathbf{P}_n)$$

$$\times \exp\left\{-\beta(\mathbf{X}_{N-n}) \sum_{i=1}^{N} \left[\frac{\mathbf{p}_i^2}{2m} + \frac{1}{N}\phi(\mathbf{x}_i, \mathbf{X}_{N-n})\right]\right\} \tag{B.6}$$

Next, we consider the effect of the boundary: With repelling boundary conditions $\varepsilon N^2 - \Phi(\mathbf{X}_{N-n})$ has a unique maximum at $\bar{\mathbf{X}}_{N-n}$ which dominates the integrand of $\int d\mathbf{X}_{N-n}$ with correction terms of order e^{-N} (we avoid critical values of the energy where phase transitions might occur). With periodic boundary conditions, for each maximum of $\varepsilon N^2 - \Phi(\mathbf{X}_{N-n})$ at $\bar{\mathbf{X}}_{N-n}$ there is a maximum at $\bar{\mathbf{X}}_{N-n} + \mathbf{a}$ as well, where $\mathbf{a}$ is an arbitrary two-dimensional vector in the configuration space of a single particle. But apart from this translational invariance, the maximum is unique: $\beta(\mathbf{X}_{N-n} + \mathbf{a}) = \beta(\mathbf{X}_{N-n})$. For a fixed maximizing $\bar{\mathbf{X}}_{N-n}$ we define

$$\lim_{N\to\infty} \phi(\mathbf{x}_i, \bar{\mathbf{X}}_{N-n}) \frac{1}{N} = \bar{\phi}(\mathbf{x}_i)$$

Furthermore,

$$\lim_{N\to\infty} \sum_{i,j=1}^{n} v(\mathbf{x}_i, \mathbf{x}_j) \frac{1}{N} = 0$$

For repelling boundaries one finally obtains from (B.3) and (B.6)

$$\rho_n(\mathbf{X}_n, \mathbf{P}_n) = \lim_{N\to\infty} c_{N,n} \int d\mathbf{X}_{N-n} [\varepsilon N^2 - \Phi(\mathbf{X}_{N-n})]^{N-n-1}$$

$$\times \sum_{i=1}^{n} \exp\left\{-\beta\left[\frac{\mathbf{p}_i^2}{2m} + \bar{\phi}(\mathbf{x}_i)\right]\right\}$$

which—together with the necessary normalization conditions for the various densities ρ_n—proves (B.1).

For periodic boundary conditions one finds accordingly

$$\rho_n(\mathbf{X}_n, \mathbf{P}_n) \sim \int d^2a \int d\mathbf{X}_n \, d\mathbf{P}_n \, f(\mathbf{X}_n, \mathbf{P}_n) \prod_{i=1}^{n} \exp\left\{-\beta\left[\frac{\mathbf{p}_i^2}{2m} + \bar{\phi}(\mathbf{x}_i - \mathbf{a})\right]\right\}$$

$$\equiv \int d^2a \, \omega_a(f)$$

The distribution contributing to $\omega_a(f)$ factorizes again and—for a given $\mathbf{a}$—the equality $S_B(\mathbf{a}) = S(\mathbf{a})/N$ holds in the limit $N \to \infty$.

ACKNOWLEDGMENTS

The extensive numerical computations were carried out within the framework of IBM's European Supercomputer Initiative in collaboration with the computer center of the University of Vienna. The project was also supported by the Austrian Fonds zur Förderung der Wissenschaftlichen Forschung, grant no. P8003.

REFERENCES

1. W. Thirring, *Z. Phys.* **235**:339 (1970).
2. P. Hertel and W. Thirring, *Ann. Phys.* (N.Y.) **63**:520 (1971).
3. H. A. Posch, H. Narnhofer, and W. Thirring, *Phys. Rev. A* **42**:1180 (1990).
4. A. Compagner, C. Bruin, and A. Roelse, *Phys. Rev. A* **39**:5089 (1989).
5. H. A. Posch, H. Narnhofer, and W. Thirring, in *Simulation of Complex Flows*, NATO Advanced Study Institute, Series B: Physics, Vol. 236, M. Mareschal, ed. (Plenum, New York, 1990), p. 241.
6. F. H. Stillinger, *J. Stat. Phys.* **23**:219 (1980).
7. E. T. Jaynes, *Phys. Rev. A* **4**:747 (1971).
8. H. A. Posch, H. Narnhofer and W. Thirring, "Condensation Phenomena in Thermodynamically Unstable Systems—A Simple Model for the Formation of Stars," Film (16 mm) and Video (U-matic), Österreichisches Bundesinstitut für den wissenschaftlichen Film, Schönbrunner Strasse 56, A-1050 Wien, Austria, Catalog No. C2337 (1990).
9. W. Thirring, *Quantum Mechanics of Large Systems, A Course in Mathematical Physics*, Vol. 4 (Springer, New York, 1980).
10. O. Bokhove and A. Compagner, in *Computational Physics and Cellular Atomata*, A. Pires, D. P. Landau, and H. Herrmann, eds. (World Scientific, Singapore, 1990), p. 179.
11. W. F. van Gunsteren and H. J.-C. Berendsen, *Mol. Phys.* **34**:1311 (1977).
12. E. T. Jaynes, *Am. J. Phys.* **33**:391 (1965).
13. S. Ma, *J. Stat. Phys.* **26**:221 (1981).
14. W. Pusz and S. L. Woronowicz, *Commun. Math. Phys.* **58**:273 (1978).
15. A. Lenard, *J. Stat. Phys.* **19**:575 (1978).
16. B. L. Holian, W. G. Hoover, and H. A. Posch, *Phys. Rev. Lett.* **59**:10 (1987).
17. H. A. Posch, W. G. Hoover, and B. L. Holian, *Ber. Bunsenges. Phys. Chem.* **94**:250 (1990).
18. R. Tolman, *The Principles of Statistical Mechanics* (Oxford University Press, Oxford, 1938).